Preliminary Estimates of the Residual Dose in the Vicinity of the First Doublet Following Machine Shutdown

BNL/SNS TECHNICAL NOTE

NO. 083

H. Ludewig, N. Catalan-Lasheras, N. Simos, A. Mallen,
J.Walker, J.Wei, M. Todosow

December, 1999

COLLIDER ACCELERATOR DEPARTMENT
BROOKHAVEN NATIONAL LABORATORY
UPTON, NEW YORK 11973

PRELIMINARY ESTIMATES OF THE RESIDUAL DOSE IN THE VICINITY OF THE FIRST DOUBLET FOLLOWING MACHINE SHUTDOWN

H. Ludewig, N. Catalan-Lasheras, N. Simos, A. Mallen, J. Walker, J. Wei, and M. Todosow.
Brookhaven National Laboratory, Upton, New York, USA. 11973.

Introduction

In this report an estimate of the residual dose in the vicinity of the first doublet, following machine shutdown will be made. A period of 4 hours following machine shutdown will be allowed for decay of short lived radio-nuclides. The activity of most components drops by approximately 30% in the first 4 hours and then drops more gradually with time. Following one month of shutdown the activity has decreased to approximately a quarter of its original value. These estimates will be carried out based on the activation of the corrector magnet, doublet, vacuum chamber wall, and the two adjoining collimators. Residual activity due to gamma-ray sources in these components will be determined at both radial (the surface of the vacuum chamber (10 cm from the beam centerline), 50 cm, and 100 cm from the beam centerline), and longitudinal (four positions along beam line) locations adjacent to the machine.

In all the above calculations the machine is assumed to operate at an average power of 2 MW, with a proton energy of 1 GeV, and a loss fraction of 0.001. It was assumed that the loss occurs on the scraper situated in the primary collimator. If the loss fraction is different from the assumed value the dose will change, but only in magnitude.

In the following sections the model and method of analysis will be described, and the dose estimates will be presented.

Methods and Modeling

The above dose estimates are based on the MCNP/LAHET [1,2] family of codes. Due to the need to link to other codes the residual activation determination was made using the LAHET codes for particles above 20 MeV; and MCNP for particles below 20 MeV. In addition, a suitably modified version of the ORIGEN [3] code was used tocalculate the buildup of spallation products during machine operation, and their decay following shutdown. In addition to the variation of radioactivity with time during operation and following shutdown, the ORIGEN code determines the variation with time of the gamma-ray spectrum of the decaying nuclides. These gamma-ray spectra are used as input to a second MCNP calculation, which only considers photons in the source description. The result of this calculation will be used to determine doses at various positions in the tunnel due to the decay gamma-ray source. This determination requires the transport of photons through the various components in the ring (collimators, magnets, and vacuum chamber walls).

In this calculational string the spallation product mass distribution is determined by the LAHET code, the averaged neutron energy spectrum in the cell of interest is determined by the first

MCNP calculation, and these two pieces of information are used to determine the appropriate nuclear cross section data and inventory of spallation products used in the modified ORIGEN code for the estimated build-up and decay of radioactive nuclides in the cell while the machine is operating and following shutdown. In this case the machine loss rate in protons/s (1.243×10^{13} protons/s lost on primary scraper) is used to determine the neutron flux, and is thus the connection to the overall machine power. In addition assumptions must be made regarding the operating time of the machine. In all these determinations it was assumed that the machine operates at full power for 180 days. In order to determine the residual activation for different times it is reasonable to scale the activity by the number of full power days. The calculational sequence described above is shown in Fig. 1. It is seen that the sequence involves several codes, and an extensive nuclear data library.

The dose estimates were made by placing point and ring detectors at the locations of interest and folding the detector response into an energy dependant dose conversion factor (ANSI/ANS-6.1.1-1977) and the total photon source (photons/s). This results in a dose in rem/hr. In addition, selected cases were checked by placing 10 cm diameter water spheres at the same locations as the point detectors, and determining the energy deposited in the spheres (MeV/gm). This quantity can be converted to rad/hr by recognizing that 1 rad=100 ergs/g, and that 1 MeV=1.602×10^{-6} ergs resulting in a conversion factor of 1.602×10^{-8}. This value must be multiplied by the total source strength in photons/s and 3600. In the case of photons the dose determined in rem/hr and rad/hr should be similar since the biological quality factor is unity regardless of photon energy, and only the energy dependant dose conversion factors used to convert flux to rem/hr could be a source of uncertainty.

The actual layout of the lattice in the collimation straight of the ring is shown in Fig. 2. From the figure it is seen that the straight section is 30 m in length, with three collimators, two sets of doublets, two quadru-poles one at each end, and two corrector magnets. The distance between the quadru-poles and the two collimators at each end is approximately 1.5 m, and the distance from the primary scraper/collimator to the corrector magnet is approximately 0.5 m. There is a comparatively long straight section between the second collimator and the second doublet (~ 12 m.), which ensures that these magnets should not be subject to the same environment as the first doublet.

The primary scraper/collimator consists of a 0.55 cm thick platinum scraper which protrudes into the halo, and perturbs the beam orbit sufficiently that the particles are deflected into one of the secondary collimators. It has been found that the scraper location must be surrounded by a substantial structure to absorb the bulk of the secondary particles generated in the scraper due to nuclear interactions, and tertiary particles generated in the structure. A fraction of this particle shower leaks out, and irradiates the down stream magnets. In these calculations it was assumed that the vacuum chamber remains unchanged in size, thus resulting in a substantial leakage path for secondary particles leaving the scraper. The second and third collimators are restrictions in the vacuum chamber and follow the beam profile at that particular location.

Dose Estimates

Estimates of the dose were carried out for the following axial and radial positions around the corrector magnet and doublet combination situated between the primary scraper/collimator and the secondary collimator.

Table 1 - Location of dose estimate detectors

Number	Radial position	Axial position	Axial Location
1	10.0	334.0	Between first collimator and
2	50.0	334.0	corrector magnet
3	100.0	334.0	
4	10.0	401.0	Between corrector magnet and
5	50.0	401.0	first quadru-pole of doublet.
6	100.0	401.0	
7	10.0	507.5	Between first quadru-pole of
8	50.0	507.5	doublet and second quadru-pole
9	100.0	507.5	of doublet.
10	10.0	606.5	Between second quadru-pole of
11	50.0	606.5	doublet and secondary collimator.
12	100.0	606.5	

The radial positions vary from the surface of the vacuum chamber (r=10.0 cm) to a position 1 m away from the beam centerline.

An estimate of the dose due to the decay gamma-ray source was made at the twelve locations described above. In addition, two configurations involving moveable shielding placed at right angles to the beam direction were considered. The first assumed a full thickness (assumed to be 20 cm of lead) moveable shield in front of the primary scraper/collimator, in this way the contribution from the primary collimator face is essentially eliminated. The second configuration considered two arm thickness pieces (each is assumed to be 5 cm thick lead) of the moveable shield in front of the primary scraper/collimator, and behind the corrector magnet. This configuration greatly reduces the contributions from both the collimator face and the magnet end. The primary contribution is from the vacuum chamber wall and the contribution scattering off the walls which originates in either the corrector magnet or the primary scraper/collimator. In both configurations the moveable shield is assumed to be disc shaped with a diameter of 220 cm. These configurations are shown in Fig. 3 -5. The axial locations referred to above in the table are also shown on these figures. The results from the above analysis is given below in Table 2.

These results indicate that the dose along the vacuum chamber wall (possible location of

flanges) is approximately 250 rem/hr, and drops off rapidly to approximately 7 rem/hr at 1 m. In addition,
the above results indicate that doses along the vacuum chamber surface are reduced by approximately a factor of two by the presence of moveable shielding in the configurations discussed. The reduction following the inclusion of a moveable shield is greater with increasing distance from the vacuum chamber wall. The effect of the two different moveable shield configurations is greatest for location 3, resulting in a dose of 1.6 rem/hr. In this case the vacuum chamber wall plays a reduced role, since it is 90 cm away, and the more efficient shielding of two surfaces in one case versus only shielding a single source in the other case. It is seen that the dose is approximately half the dose with two moveable arms compared to the case with full shielding along one wall.

Table 2 - Dose at various locations around the first corrector/doublet combination for three configurations
(Dose in rem/hr)

Number	No moveable shield Fig. 3	Full moveable shield Fig. 4	Two moveable shield arms Fig. 5
1	263.7	147.7	146.5
2	25.8	7.85	6.32
3	9.5	3.0	1.6
4	270.1	149.7	147.3
5	20.2	9.81	9.58
6	8.3	3.44	3.18
7	206.0	111.7	111.5
8	15.6	9.8	9.6
9	5.9	2.9	2.9
10	167.5	91.2	89.7
11	17.8	9.9	9.9
12	6.5	3.5	3.5

In addition to the above configurations an arrangement of moveable shielding was investigated which placed it parallel to the beam direction in front of the magnets. In this manner the direct shine off the magnets and vacuum chamber wall could be shielded. The configurations are shown on Figs. 6 and 7. In Fig. 6 the shield is seen to extent to the middle of the doublet, and in Fig. 7 the shield extends the entire distance between the primary scraper/collimator face to the secondary collimator face. Fig. 8 shows a view of the moveable shield location relative to the magnets, and also indicates its height and position relative to the floor. In the second case (Fig.7), any dose experienced behind the shield must be due to reflection (walls, tunnel air etc.),

and off the collimator shield faces.

As a check of the consistency of the estimate two types of detector were used at selected locations. The detectors considered were point detectors and ring detectors. A ring detector averages the response over its entire circumference, and thus is not sensitive to azimuthal variations in the dose at a particular radius, while the point detector only determines the response at a particular point. For a given number of particle histories, the ring detector will always give better statistics than the point detector. Finally, ring detectors are not used if the detector circumference cuts through more than one material zone. The results of these estimates are given below:

Table 3 - Dose behind shield placed parallel to beam direction
Dose in (rem/hr)

Number	Position (r,z)	Part length shield Fig. 6	Full length shield Fig. 7
	10.1, 334.0	283.56	246.27
4	10.1, 401.0	258.97	261.19
7	10.1, 507.5	199.30	196.76
8	50.0, 507.5	15.29	
9	100.0, 507.5	5.26	
10	10.1, 606.5	164.47	164.0
11	50.0, 606.5	17.78	
12	100.0, 606.5	6.33	
	(x,y,z)		
2'*	52.1, 0.0 334.0	1.88	2.04
3'	100.0, 0.0 334.0	1.57	1.64
5'	52.1, 0.0, 401.0	0.57	0.56
6'	100.0, 0.0, 401.0	0.86	0.6
8'	52.1,0.0,507.5	12.4	0.51
9'	100.0, 0.0, 507.5	4.0	0.53
11'	52.1, 0.0 606.5	16.0	2.55
12'	100.0, 0.0, 606.5	6.0	2.15

* Primed location numbers refer to point detectors

The dose along the vacuum chamber surface (r=10 cm) is consistent with the values shown in Table 2. Introduction of the moveable shields parallel to the beam direction is seen to reduce the dose by approximately an order of magnitude closest to the faces of the collimators, and close to a factor of 50 at intermediate locations. It should be noted that the dose closest to the collimator faces is due to the residual activity of the front and back shields surrounding the collimators. However, the dose at significant distances from the collimators is due to the reflection off the

walls, floor, and ceiling. It is thus essentially impossible to reduce the dose to vanishingly small values, since the accelerator components will always be irradiated, and the resulting gamma-ray source will be reflected from the concrete structures. This dose level is seen to be 0.6 rem/hr. Furthermore, by comparing positions (8 vs. 8', 9 vs. 9', 11 vs 11', 12 vs. 12' for Fig.6), where the dose was determined by both detector types (point and ring) it is seen that the values are indeed acceptably close, confirming the consistency of the estimated dose.

Finally, the dose estimate using water spheres instead of point detectors, as described above was also carried out. In this method the energy deposited in each sphere is calculated and then converted to rad/hr by an appropriate conversion factor. The location of the water spheres is shown on Fig. 9, and is identical to the point detector locations. In the conventional way of determining dose at a location the response of a point detector is folded into a dose conversion factor which yields the dose in rem/hr. Since the only source of radiation in this calculation is gamma-rays, which have a quality factor of unity, these two independent methods should in principle yield similar result. A comparison of the dose at the same locations determined by these two methods is given below.

Table 4 - Comparison of point detector and energy deposition method of determining dose

Location (x,y,z)	Point detector method (rem/hr)	Energy deposition method (rad/hr)
52.1.0.0,334.0	2.04	1.80
100.0,0.0,334.0	1.64	1.08
52.1,0.0,401.0	0.56	0.49
100.0,0.0,401.0	0.6	0.38
52.1,0.0,507.5	0.51	0.38
100.0,0.0,507.5	0.53	0.44
52.1,0.0,606.5	2.55	2.49
100.0,0.0,606.5	2.15	1.52

The statistical accuracy to which the above calculations were carried out to was approximately 10%. Thus, comparing the above two sets of results it is seen that they are close. However, in all cases it is seen that the "Point detector method" yields higher values than the "Energy deposition method", suggesting that the difference is systematic rather than statistical. A possible source for this systematic variation is the choice of dose conversion factor. The evaluation used here (ANSI/ANS-1977) is significantly higher (~ 20% below 0.7 MeV) than the other choice available (ICRP-2) in the MCNP code package. Thus, a different choice of dose conversion factor should improve the agreement, since most photons have energies below 1 MeV. This agreement between two methods of determining the same value validates the calculations of dose using point detectors.

Conclusions

1) The results reported in this study are a strong function of the assumptions regarding loss

fraction, average power and full power operating time. It was assumed that the loss fraction on the face of the scraper is 0.001 of the beam, the accelerator operated at an average power of 2 MW in an un-interrupted fashion for 180 days. The effect of any variation from these assumptions can be obtained by scaling (within limits),
2) The dose level in the tunnel following machine shutdown can be reduced by the use of moveable shielding, but refection off the walls determines the lower level of the dose operators will be exposed to, and
3) Once a firmed up design is established these estimates can be repeated for realistic loss patterns, operating profiles, and power levels.

References

1) *MCNPX Users Manual - Version 2.1.5*, L.S. Waters, ed., Los Alamos National Laboratory, Los Alamos, NM, TPO-E83-G-UG-X-00001 (1999)
2) R.E. Prael and H. Lichtenstein, *"User Guide to LCS: The LAHET Code System"*, Los Alamos National Laboratory, Los Alamos, NM, LA-UR-89-3014 (1989).
3) *MCNP-A General Monte Carlo N-Particle Transport Code Version 4A*, J.F. Breismeister, ed., Los Alamos National Laboratory, Los Alamos, NM, LA-12625-M (1993).
4) A.G. Croff, *"ORIGEN2 - A Revised and Updated Version of the Oak Ridge Isotope Generation and Depletion Code"*, Oak Ridge National Laboratory, Oak Ridge, TN, ORNL-5621 (1980).

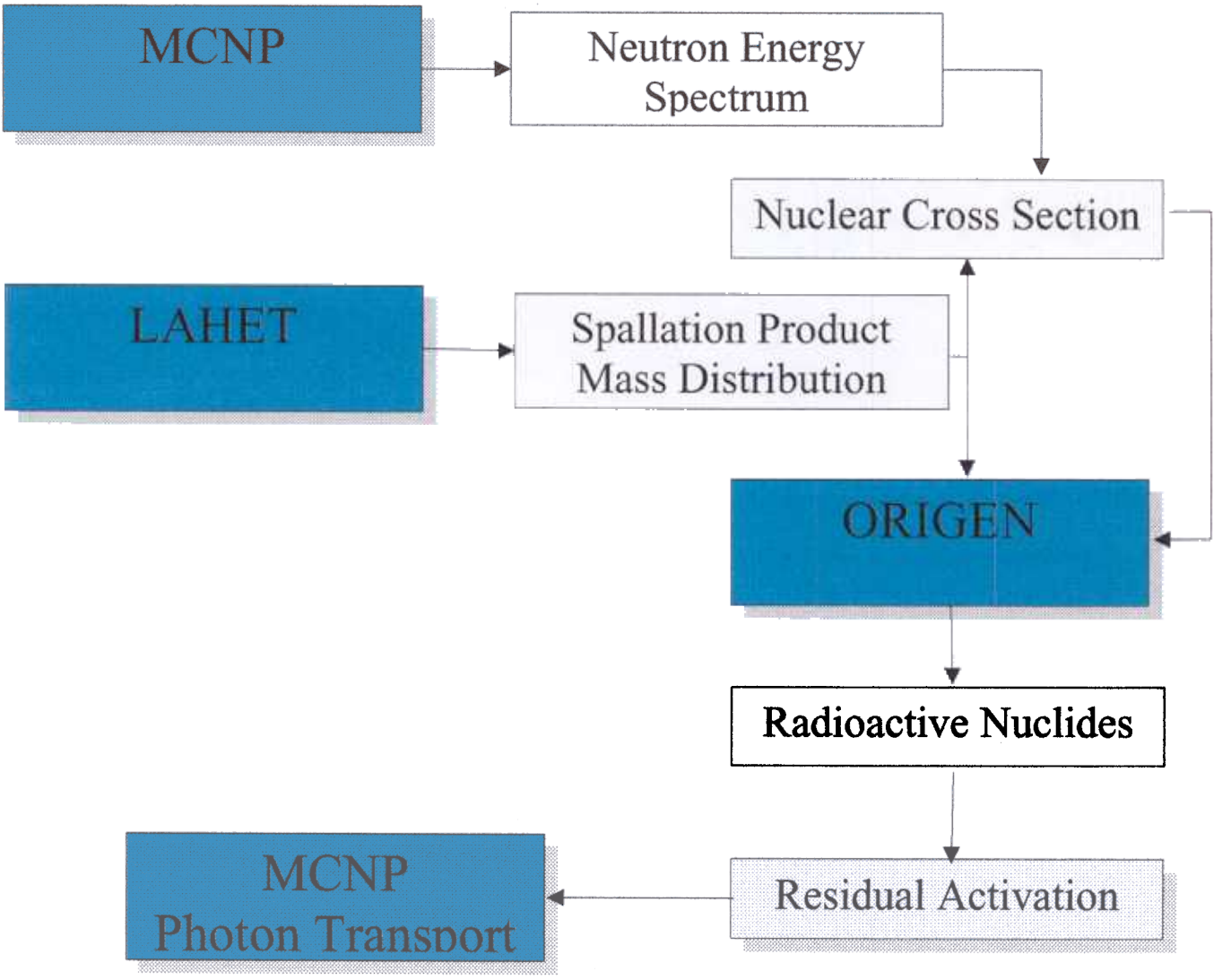
MCNP
Neutron Energy Spectrum
Nuclear Cross Section
LAHET
Spallation Product Mass Distribution
ORIGEN
Radioactive Nuclides
MCNP Photon Transport
Residual Activation

FIG 2 - COLLIMATION STRAIGHT

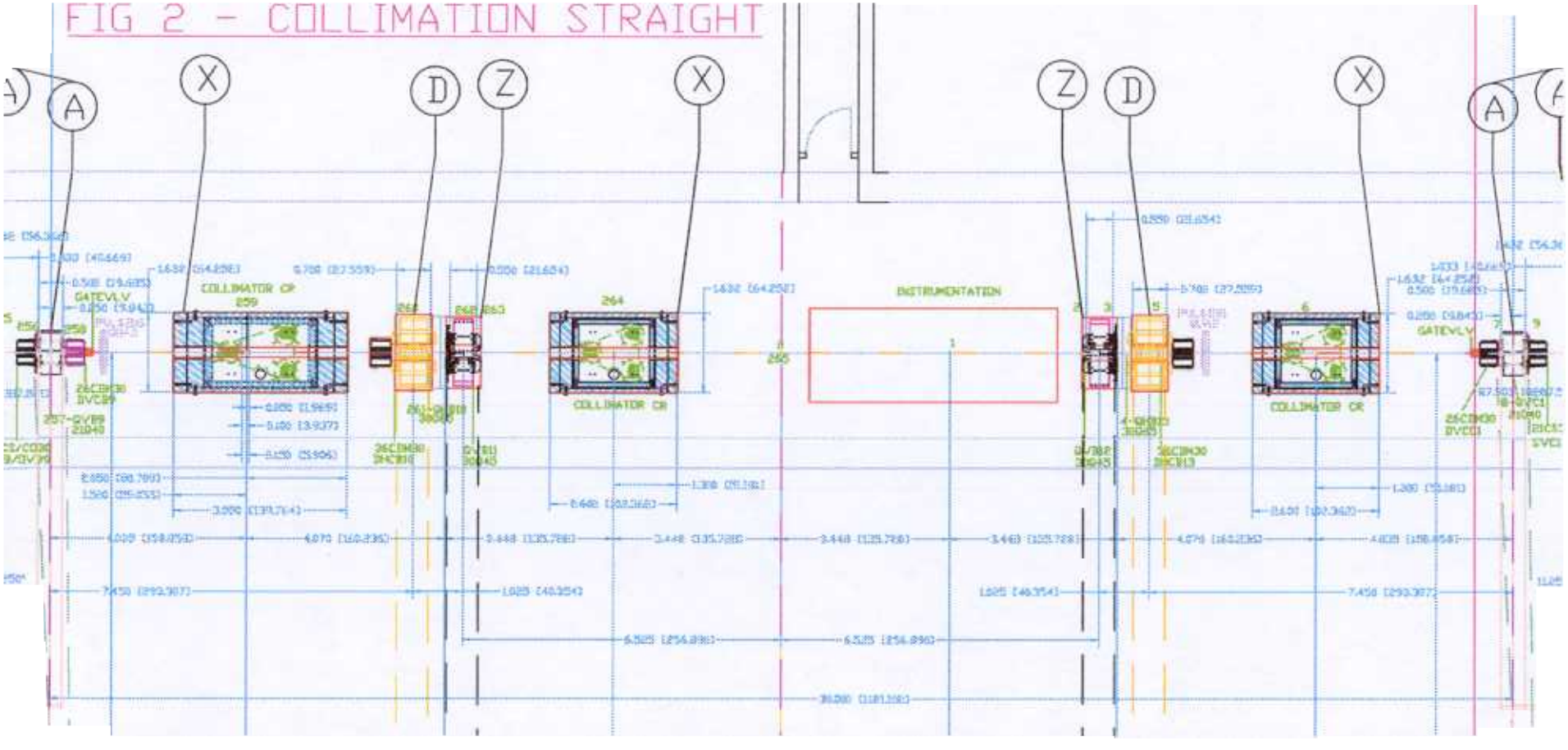

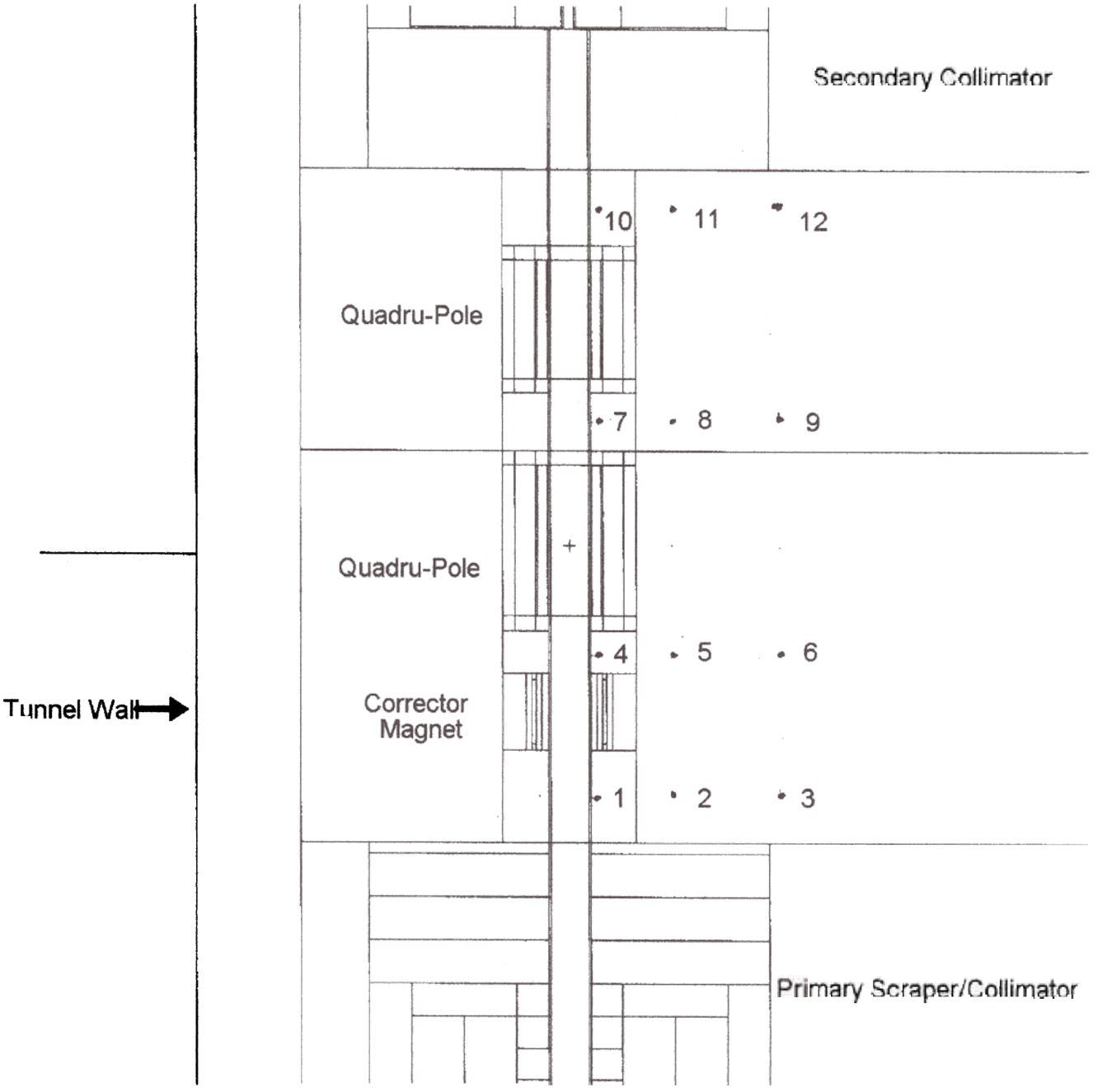

Fig 3: Locat of Detector No Moveable hield

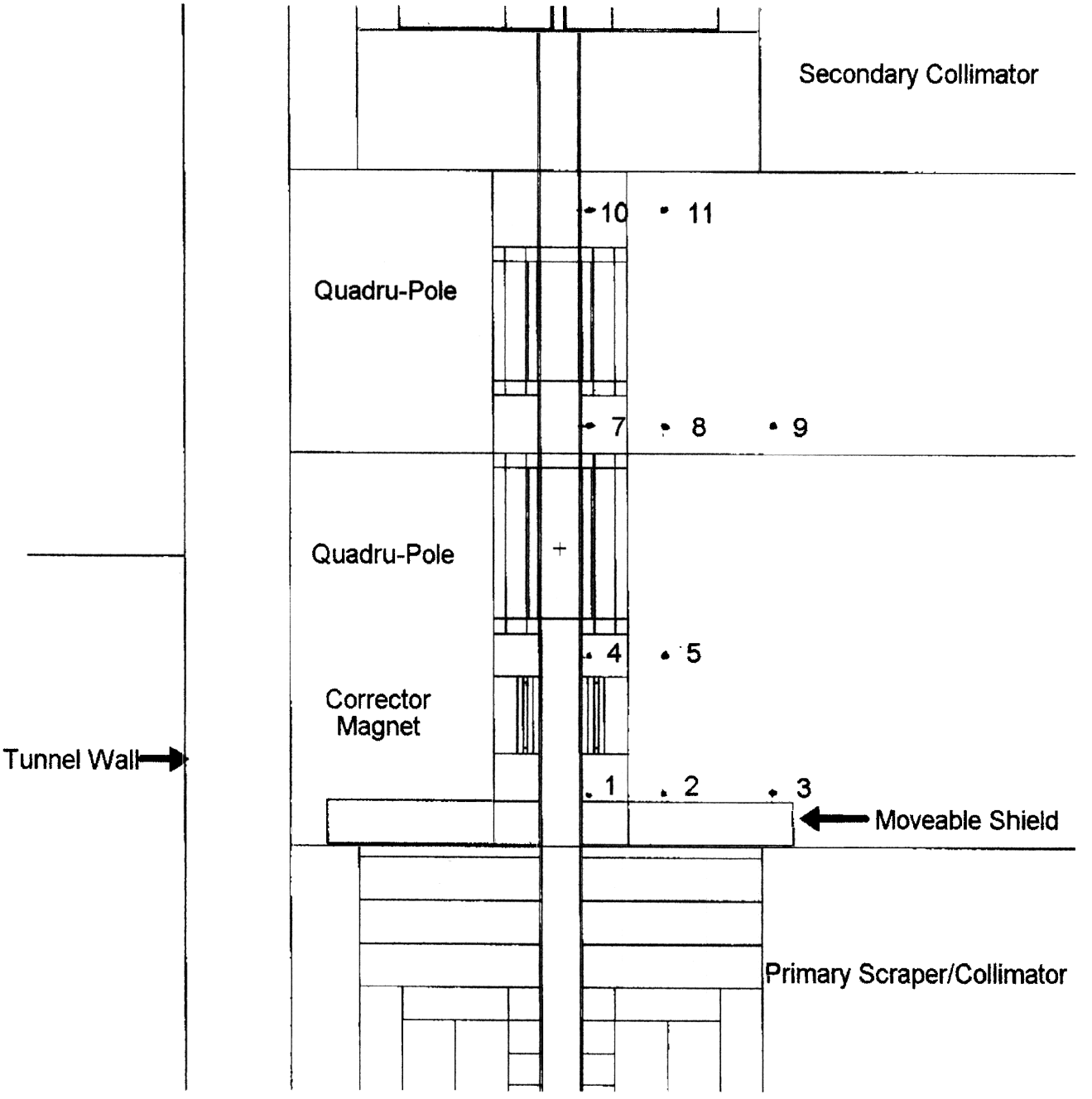

Figure 4: Location of Detectors - Moveable Shield in Front of Primary Scraper/Collimator

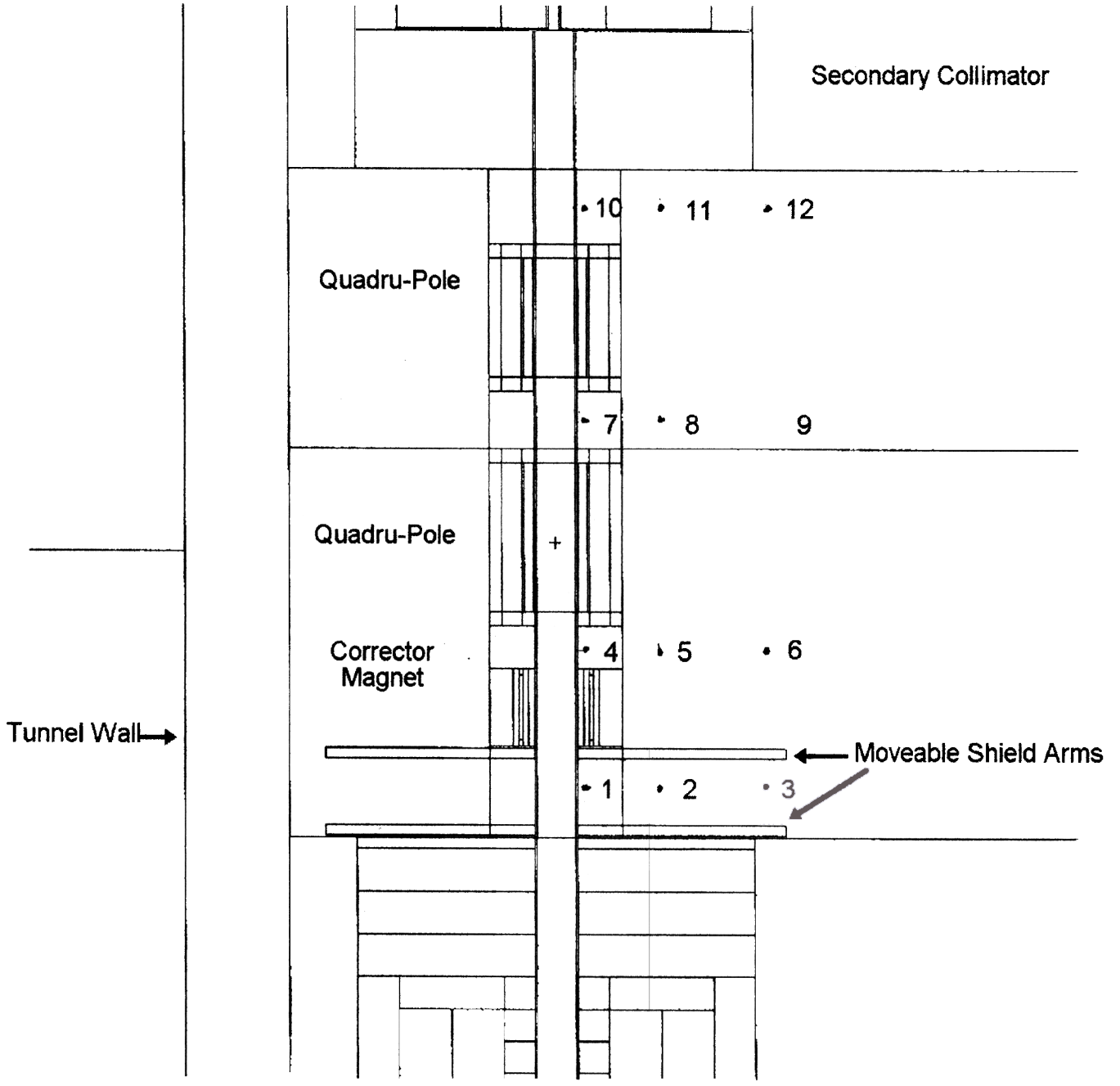

Figure 5: Location of Detectors - Two Moveable Shield Arms Covering Corrector Magnet and Primary Scraper/Collimator

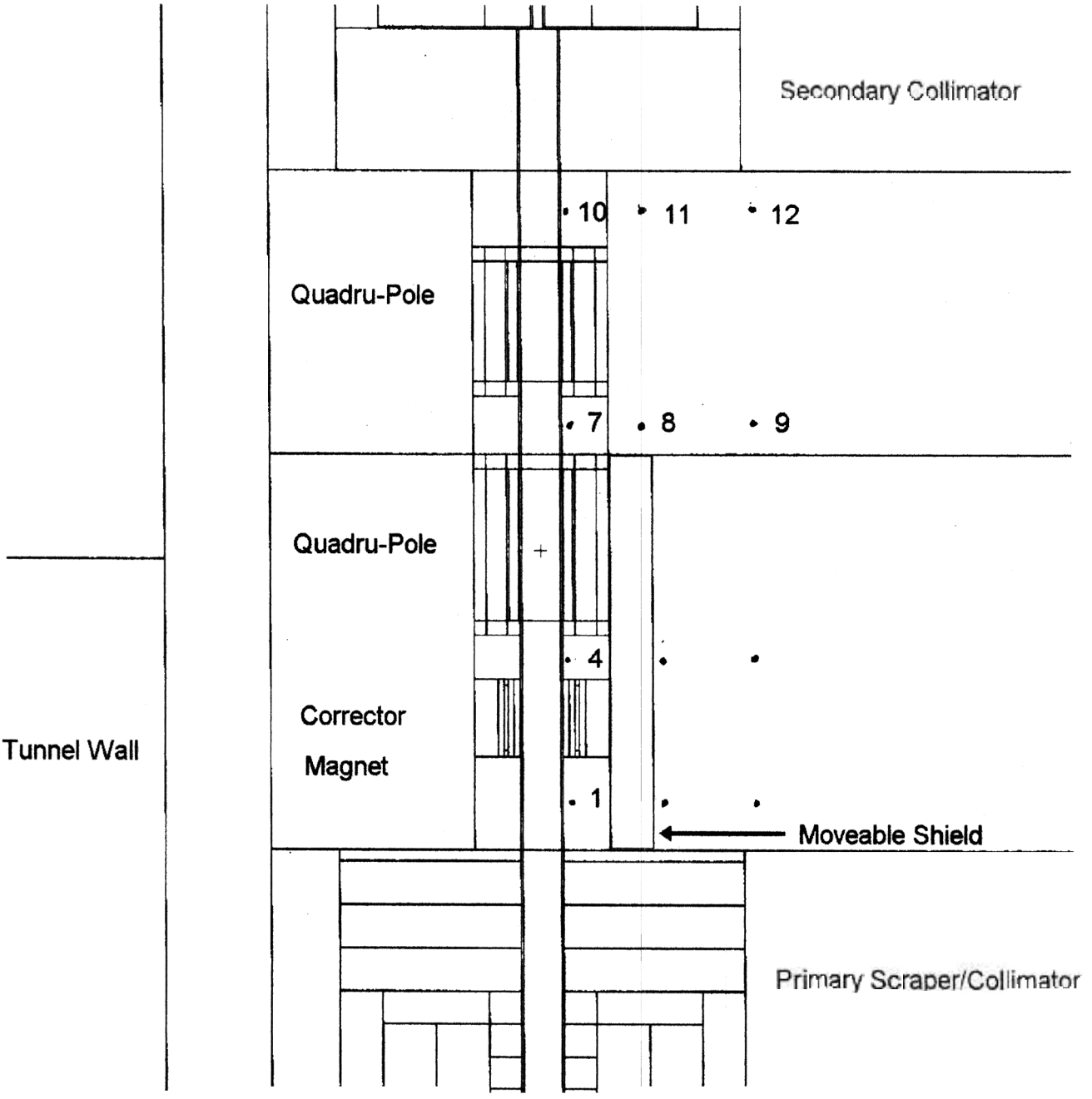

Fig 6: Location of Detectors Moveable Shield parallel to Beam Direction Part Length)

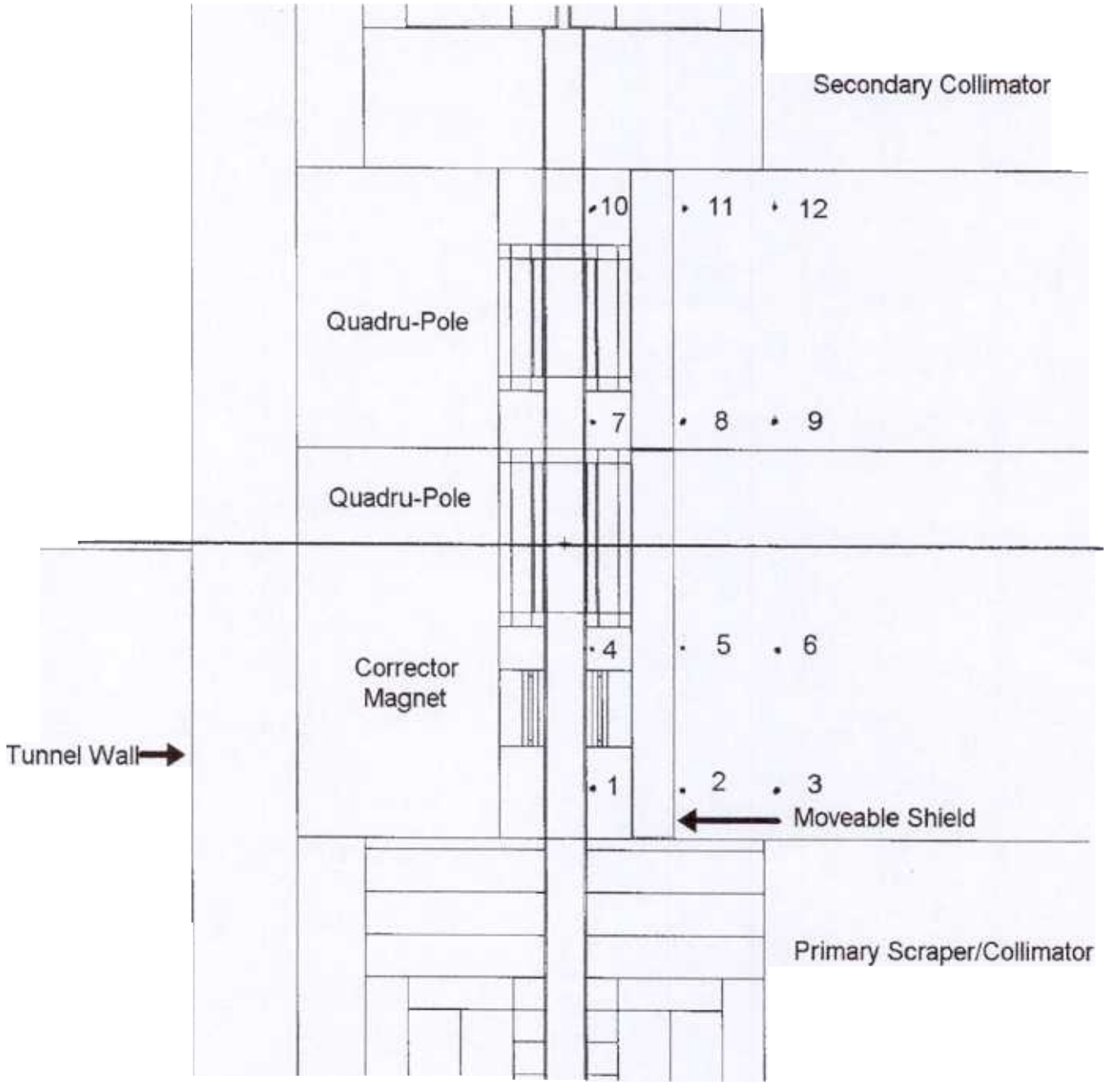

Figure 7: Location of Detectors - Moveable Shield Parallel to Beam Direction (Full Length)

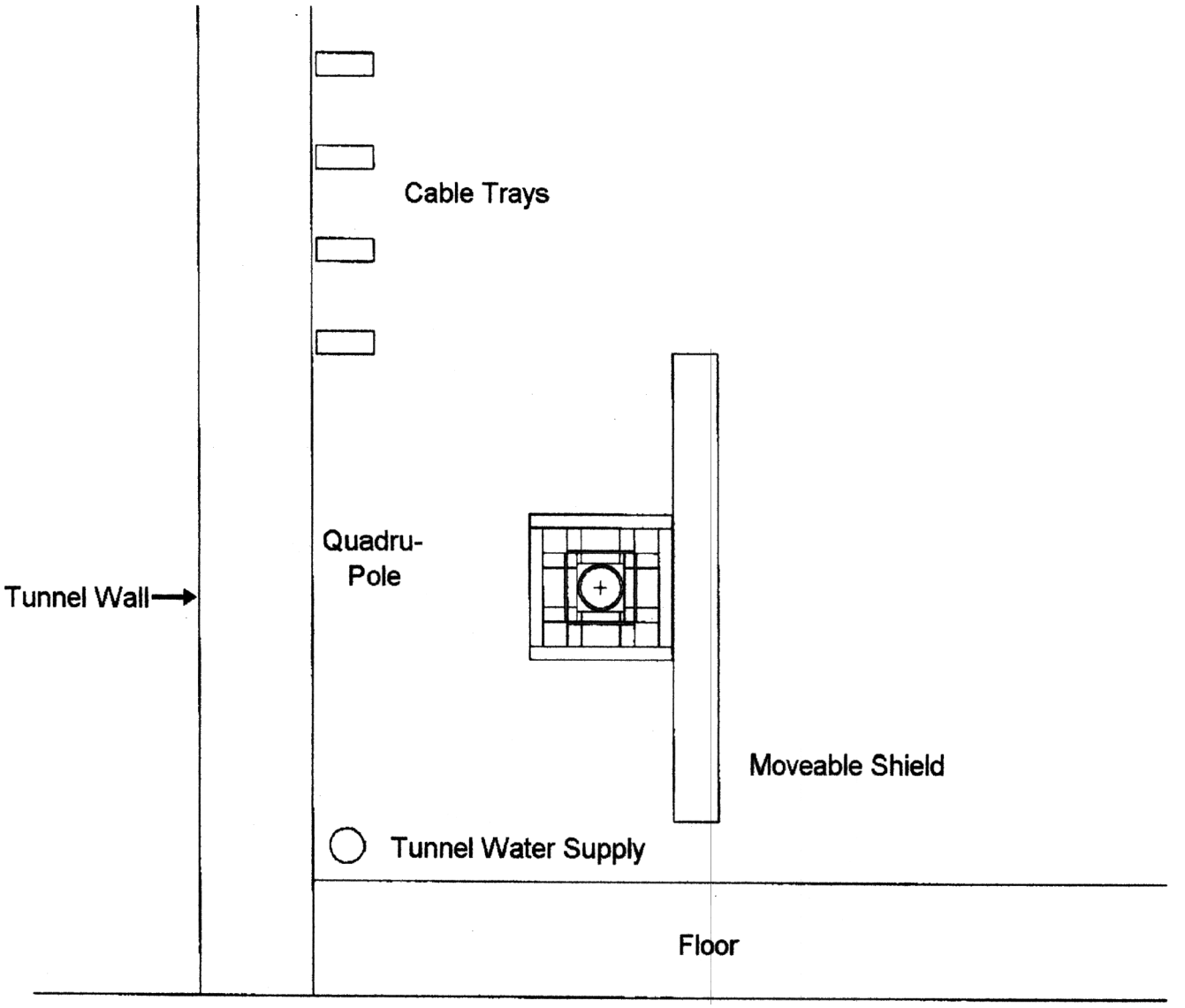

Figure 8: Section A-A Location of Moveable Shield Relative to Quadru-Pole Magnet and Beam Line

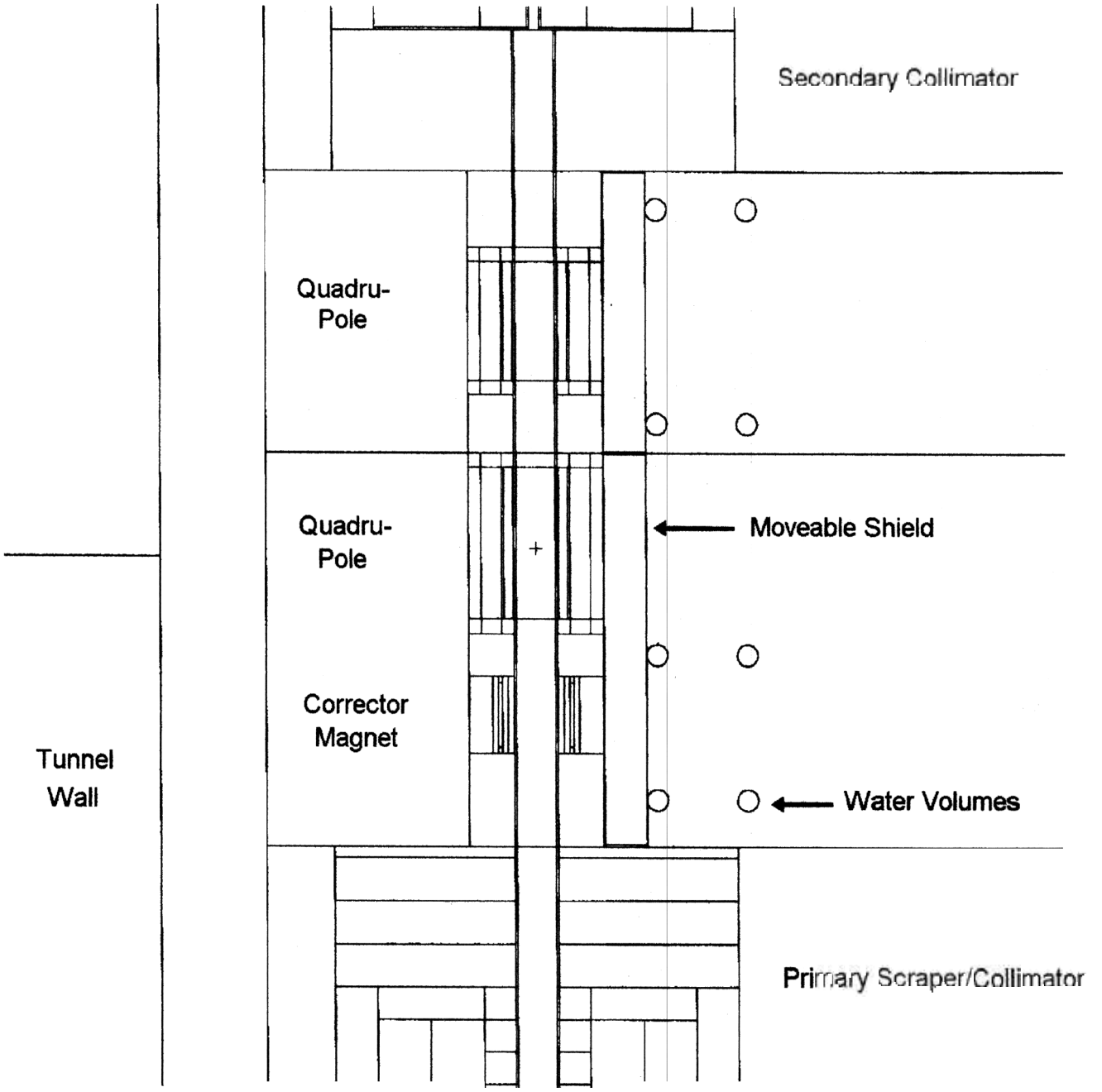

igure 9: Location of Water Volumes for Energy Deposition stimate